



Contents lists available at ScienceDirect

Journal of Photochemistry and Photobiology A: Chemistry

journal homepage: www.elsevier.com/locate/jphotochem

Novel photopolymerizations initiated by alkyl radicals generated from photocatalyzed decarboxylation of carboxylic acids over oxide semiconductor nanoparticles: Extended photo-Kolbe reactions

Zhen Weng, Xiuyuan Ni*, Dan Yang, Jiao Wang, Weikang Chen

The Key Laboratory of Molecular Engineering of Polymer of Minister of Education, Department of Macromolecular Science, 220 Handen Road, Fudan University, Shanghai 200433, China

ARTICLE INFO

Article history:

Received 30 December 2007
Received in revised form
19 September 2008
Accepted 22 October 2008
Available online 5 November 2008

Keywords:

Photopolymerization
Photo-Kolbe reaction
Photocatalysis
Semiconductor nanoparticle
Carboxylic acid

ABSTRACT

Polymerizations of vinyl acetate are photocatalyzed by TiO₂ nanoparticles in presence of carboxylic acids including propionic acid, n-butyric acid and pivalic acid. Nuclear magnetic resonance (NMR) analysis using ¹³C-labeled n-butyric acid as the probing molecule demonstrates that the polymerization of vinyl acetate is initiated by alkyl radicals generated from photocatalytic decarboxylation of the carboxylic acid. A universal mechanism is established with extending the photo-Kolbe reaction from acetic acid to the carboxylic acids with longer chains. Kinetics studies find that n-butyric acid has higher initiation rate than acetic acid, indicating more efficient decarboxylation for butyric acid than acetic acid in their aqueous solutions. It is proved that carboxylates participate in the decarboxylation. Attenuated total reflection Fourier-transform infrared (ATR-FTIR) spectra are obtained with aqueous solutions of the carboxylic acids in contact with a layer of the TiO₂ nanoparticles, and the observations are discussed with respect to the interaction between the TiO₂ and carboxylic acids.

© 2008 Elsevier B.V. All rights reserved.

1. Introduction

Photo-excitation of semiconductor nanoparticles (NPs) gives rise to electron and hole as the charge carriers that can catalyze redox reactions at the surface [1]. The photocatalysis has found broad applications associated with pollutant treatments, air disinfection, and photochemical cells [1]. Polymerizations of alkenes initiated by the photo-excited semiconductor NPs [2–6], which are called photocatalytic polymerizations, endue semiconductor NPs with a novel function. Recently, we have reported the photocatalytic polymerization of methyl methacrylate and reaction kinetics by using TiO₂ NPs [4–6]. With this method, lots of applications are envisaged such as fabricating the heterojunction nanocomposites of polymers and inorganic semiconductors. The two components can interact through the interface of large area because nanoparticles have a big surface-to-volume ratio. As the photocatalytic polymerization produces the polymer and composite in one step, it is apparent that this method has the advantage of a simplified process, in comparison with the common methods for preparing nanocomposites. Moreover, it is promising that this polymeriza-

tion can work by utilizing solar energy because the photocatalysis of semiconductor NPs is available within the spectrum of sunlight.

More recently, we have found Photo-Kolbe reaction to be a novel route to initiating polymerizations during our search for a photocatalytic polymerization of vinyl acetate with TiO₂ NPs [7]. We observed that no polymer was yielded if the aqueous solution of vinyl acetate, which was freshly prepared, was used instantly, but the polymerization came true when we happened to use the solution stored for a long time [7]. Further investigations have clarified that hydrolysis of vinyl acetate produces acetic acid and the acetic acid governs this polymerization. ¹³C NMR analysis of the polymer structure has finally revealed that the polymerization of vinyl acetate is initiated by methyl radicals that are generated from β-scission (or called decarboxylation) of acetic acid [7]. Kraeutler and Bard [8,9] have reported that the photocatalyzed reaction of acetic acid over TiO₂ produces methane and carbon dioxide, suggested methyl radical as an intermediate, and named the reaction the photo-Kolbe reaction in their pioneering work. Our results solidly evidence the methyl radical intermediate from a view of point of polymerization, while utilizing acetic acid to initiate polymerizations is thus developed for the first time. Distinguished from usual photocatalytic-degradation of aliphatic acids, photo-Kolbe reaction occurred under anaerobic condition.

* Corresponding author. Tel.: +86 21 65640982; fax: +86 21 65640293.
E-mail address: xyjni@fudan.edu.cn (X. Ni).

Studies of the photo-Kolbe reaction are motivated by the fact that this reaction is a model oxidation and understanding of the mechanism enables one to put deep insight into the photocatalysis about the oxide semiconductors [10–14]. However, no definite result is reported at present for carboxylic acids with longer chain length due probably to their more complex structures than acetic acid, although arguments proposed a decarboxylation [14]. Continuing our previous work, this study addresses on the interests: whether carboxylic acids with longer chains can have the same initiating function as acetic acid, followed by how about their efficiencies in comparison with acetic acid. Various aliphatic acids are investigated including propionic acid, n-butyric acid and pivalic acid. Results decide whether or not we can establish a universal reaction mechanism and have more opportunities to achieve photocatalytic polymerizations. With the aim of understanding the interaction between the TiO₂ and carboxylic acids studied, ATR-FTIR spectra are obtained with aqueous solutions of the carboxylic acids in contact with a layer of the TiO₂ NPs. A problem in FTIR spectroscopy of aqueous systems is the strong absorption by water. The ATR technique offers conveniently short path lengths that enable subtraction of the aqueous background absorption. The high signal-to-noise of ATR-FTIR has allowed distinguishing between conformations of acetic acid on TiO₂ [15,16].

2. Experimental

The TiO₂ semiconductors NPs used was Degussa P25 (80% anatase and 20% rutile) with an average diameter of 21 nm and a surface area of 50 m²/g. 2-¹³C-butyric acid (CH₃CH₂¹³CH₂COOH) was supplied by Aldrich Co. All the chemicals used were of analytical reagent grade. Vinyl acetate (VAc) was distilled before use. Deionized water was employed in experiments.

VAc was added into water to prepare aqueous solution. Then, the powdered TiO₂ NPs were dispersed into the aqueous VAc solution using the ultrasonic dispersion technique. After an aliphatic acid is added into the suspension, 120 mL of the mixture was moved into a quartz reactor which was equipped with a magnetic stirrer and a water jacket connected to a circulator of CuSO₄ solution, and then the reactor was sealed. UV irradiation towards the reactor was carried out using a mercury vapor lamp, characterized by two chief peaks at 254 and 365 nm in its emission spectrum. The mixture can avoid being irradiated by the rays exclusive of 365 nm, due to the cutting off of CuSO₄ solution [4]. The light intensity was measured by radiometry (UV-A, BJNU photoelectrical Co.) to be 13 mW/cm² at the frequency of 365 nm which was employed in the experiments, and only 0.085 mW/cm² at 254 nm. The irradiation lasted for different time. The precipitations were obtained by centrifugation of the reacted mixture, washed by water, and then dried under vacuum for 24 h at room temperature.

The concentrations of vinyl acetate in the reactor were measured by Gas Chromatography (GC-960, Haixin). Thermogravimetry analysis (TGA) of the products was carried out on a Perkin Elmer Pyris 1 TGA instrument in air atmosphere. ¹³C NMR spectra were recorded on a Bruker DMX500 spectrometer at 300 K using CDCl₃ as solvent. ATR-FTIR spectra were recorded a NEXUS-470 spectrometer. The upper surface of the ATR crystal was coated with TiO₂ layers by applying 100 μL aqueous suspension of the TiO₂ nanoparticles (20 mg/mL), followed by air drying. A typical experiment was started with 2.5 mL 0.01 M KCl aqueous solution at the same pH of the subsequent measurements. After the equilibration with the coated ATR surface had been reached, a blank single-beam spectrum was collected as the background spectrum. Volumes (20–50 μL) of the aqueous solution of carboxylic acid of interest were then added. The spectra were then obtained by aver-

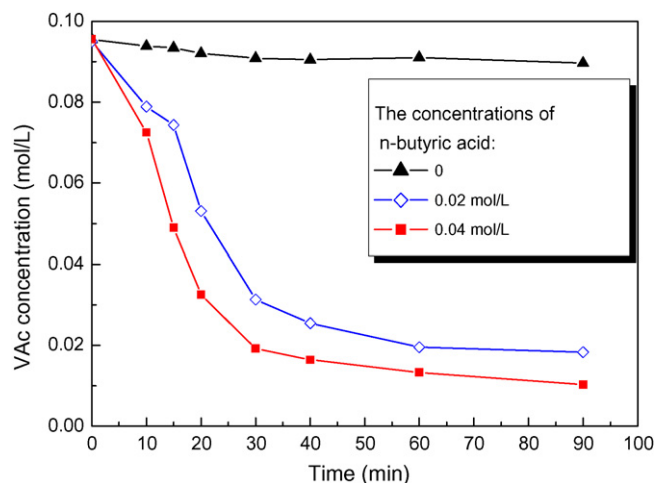


Fig. 1. The concentrations of VAc versus the reaction time. The amount of TiO₂ NPs is 1 g/L.

aging 512 scans against the appropriate background spectrum with the spectral resolution of 4 cm⁻¹.

3. Results and discussion

3.1. Reaction mechanisms

Fig. 1 shows that the concentration of VAc is sharply reduced at the early stage of the reaction then changes slowly when the reaction mixture contains n-butyric acid. It is observed that at a constant content of TiO₂ NPs, the VAc concentrations decrease faster when more butyric acid is added. This result indicates that the reaction efficiency is enhanced with an increase in the concentration of n-butyric acid. In Fig. 2 showing the TGA and differential thermogravimetry (DTG) curves of the reaction product, the thermal stage with the peak temperature at 340 °C refers to the cleavage of side acetate groups at poly (vinyl acetate) (PVAc) [17], while the weight loss occurred after 400 °C is due to the cleavage of the C–C backbones of PVAc [17]. Therefore, using butyric acid succeeds in obtaining the polymerization of VAc. It should be emphasized that the concentration of VAc keeps almost constant under the identical reaction conditions but in absence of butyric acid, as shown in Fig. 1. This result indicates that the added butyric acid governs the polymerization. As butyric acid itself never initiates any polymerization of vinyl acetate according to the principles of polymer chemistry, the polymerization is of course due to the photocatalytic reaction of butyric acid on the TiO₂ NPs.

To reveal the mechanism, the polymer structures are analyzed using ¹³C NMR spectroscopy. Fig. 3A shows the spectrum of PVAc obtained by using a ¹³C-labeled butyric acid, 2-¹³C-butyric acid (CH₃CH₂¹³CH₂COOH). This spectrum is found to accord well with that of normal PVAc [7] except a new peak at 27.2 ppm here. The intense peaks at 20.9 ppm is assigned to acetate CH₃, 38.6–39.8 ppm with several splitting bands to main-chain CH₂, 66.0–67.8 ppm to main-chain CH, and 170.2 ppm is assigned to main-chain C=O. They are totally characterized by PVAc synthesized through a free radical polymerization [18]. For the sake of clear illustration, the spectrum of PVAc synthesized by using 2-¹³C-acetic acid (¹³CH₃COOH) [7] is presented in Fig. 3 B. With the exception of a peak at 9.3 ppm, the spectrum accords well with that of normal PVAc. The peak at 9.3 ppm has been assigned to the terminal CH₃ group at PVAc [7], based on the well-known Lindeman–Adams rule [19,20]. In this study, calculations on this rule assign the new peak at 27.2 ppm to γ-CH₂ of terminal n-propyl group. The sequences of the

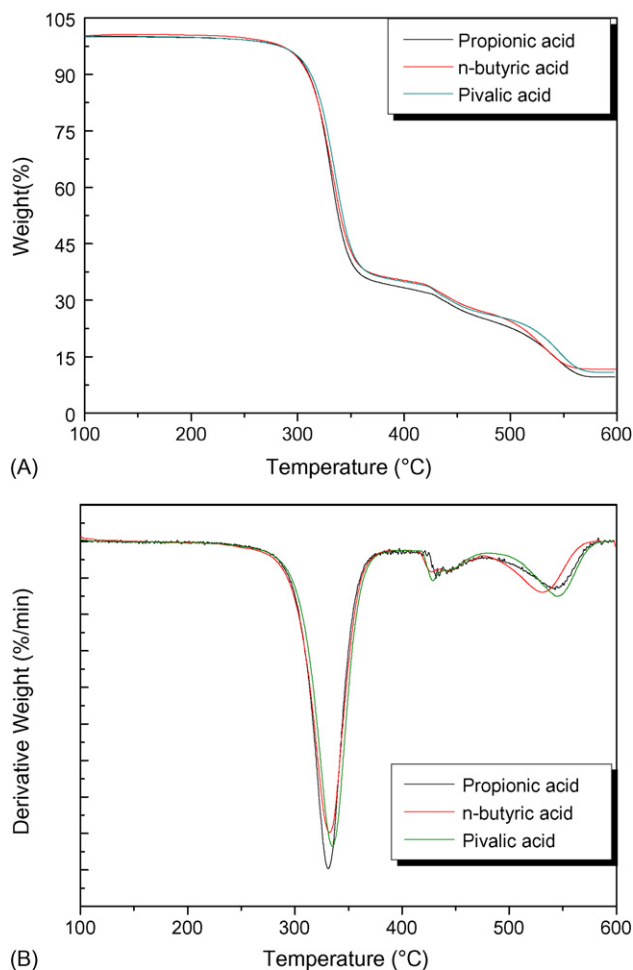
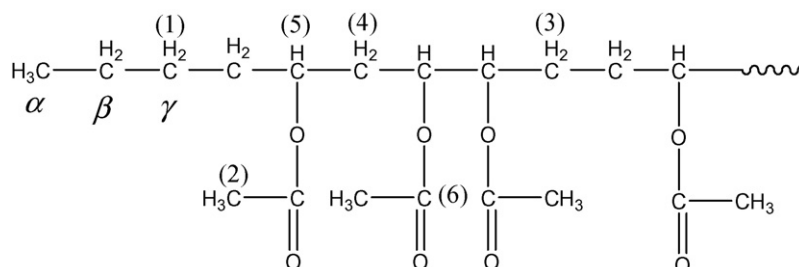


Fig. 2. TGA (A) and DTG (B) curves of PVAc obtained by adding propionic acid, n-butyric acid and pivalic acid.

polymer chain are shown in Scheme 1. In detail, Lindeman–Adams rule expresses the chemical shift of Carbon k , $\delta_c(k)$ as:

$$\delta_c(k) = \delta_c(k, RH) + \sum_i Z_{ki}(R_i) \quad (1)$$

where $\delta_c(k, RH)$ is the increment for the unsubstituted carbon atom at k position. $Z_{ki}(R_i)$ is the increment due to the substitution of R_i . From the increment database [21], it is calculated out that $\delta_c(k, RH) = 32.2$ ppm while $Z_{ki}(R_i) = -4$ ppm for γ -CH₂. So, the chemical shift of γ -CH₂ is at 28.2 ppm, being very close to the detected data. In addition, the values predicted for the other chain carbons, based on this rule, are also in good agreement with the spectroscopic data (see Table 1). As well-known, ¹³C NMR spectroscopy is



Scheme 1. The structure of PVAc synthesized by adding n-butyric acid.

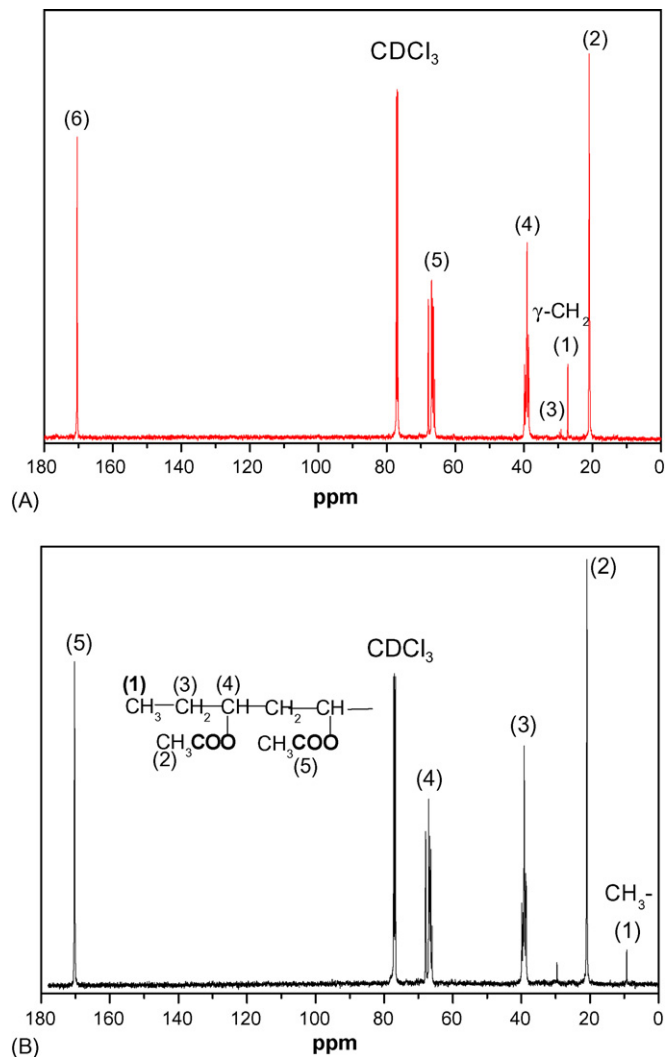


Fig. 3. ¹³C NMR spectrum of PVAc obtained by (A) adding 100 μL 2-¹³C-butyric acid and (B) adding 100 μL 2-¹³C-acetic acid. The concentration of VAc is 15 g/L. The amount of TiO₂ NPs is 1 g/L.

unable to exhibit the terminal carbon of a normal polymeric chain since the signal of the terminal carbon is too weak owing to its little fraction among the total chain-carbons. The detection of γ -CH₂ above is due to the fact that its signal is magnified by β -carbon at the ¹³C labeled butyric acid used. We therefore conclude that the polymerization of vinyl acetate is initiated by n-propyl radicals by addition reaction, and the decarboxylation (or β -scission) of butyric acid produces the n-propyl radical.

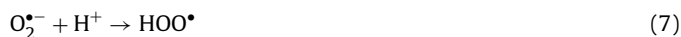
The synthesis of PVAc is also achieved by using propionic acid and pivalic acid, having the characteristic thermal behaviors as

shown in Fig. 2. However, efforts to exhibit the mechanism with ^{13}C NMR spectroscopy are not fulfilled because proper commercial ^{13}C -labeled carboxylic acids except 2- ^{13}C -butyric acid cannot be purchased. Nevertheless, the obtained results from the studies on acetic acid [7], propionic acid, butyric acid and pivalic acid are adequate for us to establish the universal mechanism for the photocatalytic polymerization as follows:



Eq. (2) represents the photo-Kolbe reaction [8,9] in the case of $\text{R}=\text{CH}_3$, while it is the only photochemical step involved in the polymerization. Once a monomer is initiated by the alkyl radicals, the adducted radical reacts with another monomer to produce a chain propagated radical and eventually the polymer.

Photo-excitation of semiconductors gives rise to conduction-band electrons (e^-) and valence-band holes (h^+) in pairs. Studies on semiconductor photocatalysis have proposed that the electrons participate into the reactions of two pathways [1]:



Indicated by reactions (6)–(8), one pathway is that the electron which is trapped by TiO_2 surface, e^-_{tr} reduces the molecular oxygen to H_2O_2 . It is apparent from the three reactions that production of 1 molar H_2O_2 will consume 1 molar O_2 . We have measured by using a dissolved-oxygen detector that the oxygen in the sealed reactor is completely consumed within 8 min once the UV-irradiation is switched on, which should be caused by the reaction of oxygen with the electron, and the reaction of oxygen with alkyl radicals. The reaction of oxygen and radicals always occurs in a free radical polymerization. As well known, the free radical polymerization does not proceed until the oxygen in the reactor is completely consumed. In absence of molecular oxygen, the photoinduced electrons have to react with Ti^{4+} ions with formation of Ti^{3+} ions as indicated by reaction (5), and the alkyl radicals initiate the monomers to polymerize without the hindering effect of oxygen.

From the phenomenon that no polymer was yielded when the aqueous solution of vinyl acetate was replaced by pure vinyl acetate, we have ratiocinated that acetate ions would play an important role in the photo-Kolbe reaction of acetic acid [7]. In order to validate the assumption, we here design the reaction by using sodium n-butyrate, which is totally ionized into n-butyrate, $\text{C}_3\text{H}_7\text{COO}^-$ in the aqueous solution. As indicated in Fig. 4, VAc polymerizes smoothly with its concentration decreasing along with the reaction. Hence, it is apparent that the carboxylate participates in the decarboxylation

Table 1
Assignments of the ^{13}C NMR peaks of PVAc in CDCl_3 solvent obtained by adding 2- ^{13}C -butyric acid ($\text{CH}_3\text{CH}_2\text{ }^{13}\text{CH}_2\text{COOH}$).

Peak	Prediction (ppm)	Spectrum (ppm)	Assignment
(1)	28.20	27.19	Ultimate $\gamma\text{-CH}_2$
(2)	21.00	20.85–21.03	Acetate CH_3
(3)	30.86	29.6	Inverted addition CH_2
(4)	39.86	38.62–39.84	Main-chain CH_2
(5)	66.90	66.70–67.90	Main-chain CH
(6)	170.3	170.32–170.44	Main-chain $\text{C}=\text{O}$

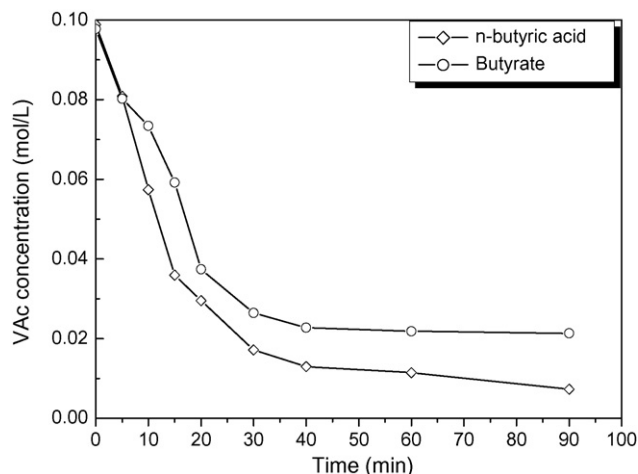


Fig. 4. The concentrations of VAc versus the reaction time. The molar concentration of both butyric acid and sodium n-butyrate is 0.03 M. The pH value of the solutions containing butyric acid and sodium n-butyrate are at 3.18 and 8.65, respectively. The amount of TiO_2 NPs added is 1 g/L.

reaction as follows:



Considering the ionization of the carboxylic acid gives RCOO^- and H^+ in pairs, the reactions in both Eq. (9) and Eq. (2) are equivalent in the aqueous system. However, this is still a challenge to clarify reaction details about the unionized RCOOH .

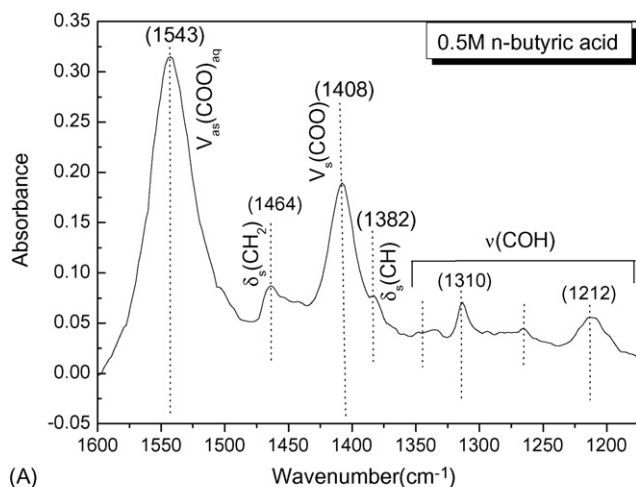
From the viewpoint of photopolymerization, the results of our study provide a novel initiating pathway by utilizing a combination of aliphatic acid and TiO_2 as the sensitizer. In general photopolymerizations are of low energy cost and rapid curing, compared to thermally induced polymerizations. The advantages have led to broad applications. However, photo-sensitizers of conventional photopolymerizations, which are often derived from acetophenone and benzoin [22], are usually water insoluble, thus most of the photopolymerizations are confined to organic solvents. The polymerization initiated by the extended photo-Kolbe reactions here is competitive since the water-born nature is urged by the environmental issue while each of the sensitizers is non-toxic and readily acquired.

3.2. Rates of initiation reaction

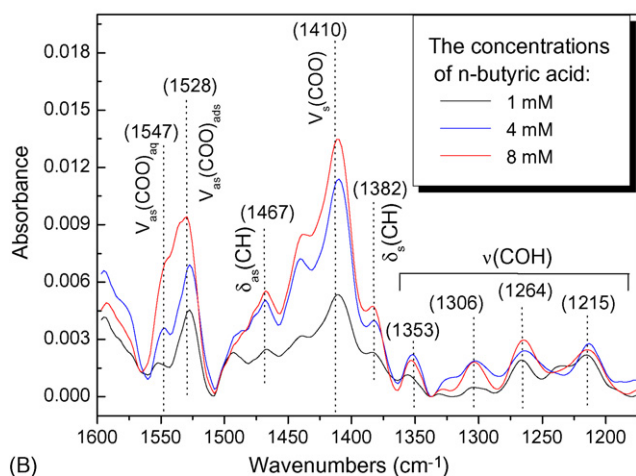
In a free radical polymerization, the kinetic chain length (ν) is defined as [23]:

$$\nu = \frac{k_p[M]}{2k_t^{1/2}R_i^{1/2}} \quad (10)$$

where k_p is the rate constant of polymerization, k_t is the rate constant of termination, $[M]$ is the molar concentration of monomer, and R_i is the initiating rate. The number-average molecular weight of polymer is known to be the kinetic chain length timing 1 or 2 depending on the types of chain terminations [23]. The ratio of NMR peak intensities for the terminal carbon to any main-chain carbon is in inverse proportion to the number-average molecular weight. In Fig. 3 showing the NMR spectra of PVAc obtained by using 100 μL acids at the same concentration of monomer, the peak intensity of the terminal carbon for using butyric acid (27.2 ppm) is found to be about two times higher than using acetic acid (9.3 ppm), by taking any main-chain carbon as the reference. It is revealed that the initiating rate is higher for using butyric acid than acetic acid, based on Eq. (10).



(A)



(B)

Fig. 5. ATR-FTIR spectra obtained with (A) the aqueous solution of n-butyric acid at pH 5.0 and (B) the aqueous solution of n-butyric acid in contact with the layer of the TiO₂ NPs at pH 5.0.

It is known that the initiating reaction of a free radical polymerization is associated with the two steps: the generation of radicals; the reaction of the radical with monomer. The rate of initiating reaction is controlled by the step of slower rate. In current photocatalytic polymerization, the generation of radicals is ruled by reaction (2), while the reaction of the radical with monomer is ruled by the kinetics equation [23]:

$$R_{\text{Addition}} = k_i[\text{R}^*][\text{M}] \quad (11)$$

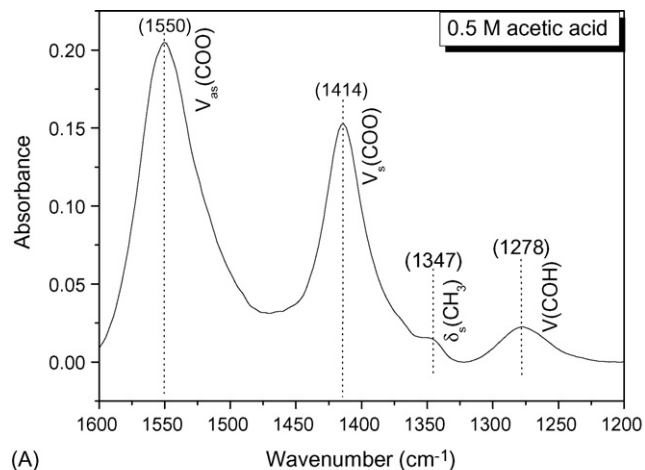
where k_i is the rate constant of the addition reaction, $[\text{R}^*]$ is the molar concentration of alkyl radicals generated. Assuming reaction (2) is the controlling step, the rate of decarboxylation must be faster for butyric acid than acetic acid so that the higher initiating rate of butyric acid can be interpreted. Szwarc and co-worker [24] have shown that the intrinsic reactivities for an addition reaction with alkenes are identical for methyl radicals and propyl radicals, so the two kinds of radicals have the same rate constant k_i . It is followed that if assuming reaction (11) is the controlling step, the molar concentration of the generated n-propyl radicals must be higher than that of methyl radicals. Therefore, the decarboxylation of butyric acid essentially behaves more efficiently than acetic acid no matter which possibility above is proved true at last.

Moreover, it is interesting to find in Fig. 4 that the monomer conversion is 90% for using butyric acid and 79% for using n-butyrate. When the acid-base equilibria at the TiO₂ surface are

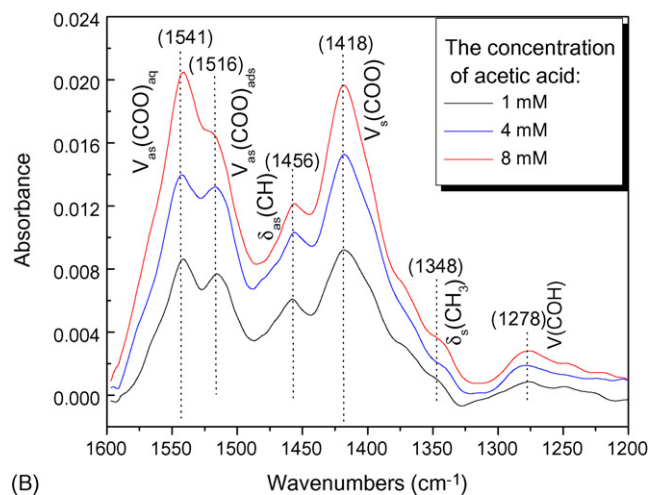
taken into consideration, this difference is interpreted by the surface interaction. Oxide semiconductor particles are amphoteric when suspended in water. In the case of TiO₂, the principal amphoteric surface functionality is the “titanol” moiety, >TiOH. The hydroxyl groups on the TiO₂ surface undergo the acid-base equilibria, giving >TiOH₂⁺ and TiO⁻ at the both sides of the reaction [1]. The pH of zero point of charge is pH_{zpc} 6.25 for Degussa P25 TiO₂ [1]. For the solution containing butyric acid at pH 3.18, the TiO₂ surface is positively charged due to $\text{pH} < \text{pH}_{\text{zpc}}$ [1], and the anionic C₃H₇COO⁻ from the ionization are absorbed by the electrostatic attraction. In contrast, the TiO₂ surface is negatively charged for the butyrate solution at pH 8.65 where $\text{pH} > \text{pH}_{\text{zpc}}$. As a result of the electrostatic interaction, C₃H₇COO⁻ should be repelled away from the TiO₂ surface. Accordingly, it is deduced that the photocatalytic decarboxylation of the carboxylic acid is probably dominated by the carboxylates.

3.3. ATR-FTIR analysis of interactions

The ATR-FTIR spectra shown in Fig. 5 are obtained for the aqueous solutions of butyric acid. To admit the interaction of carboxylate, each of the solutions is adjusted to be at pH 5.0 where $\text{pH} < \text{pH}_{\text{zpc}}$. Fig. 5A shows the spectrum of neat aqueous butyric acid obtained with an uncoated ATR crystal. The peaks at 1408 and 1543 cm⁻¹ are assigned to the symmetric $\nu_s(\text{COO})$ vibration and



(A)



(B)

Fig. 6. ATR-FTIR spectra obtained with (A) the aqueous solution of acetic acid at pH 5.0 and (B) the aqueous solution of acetic acid in contact with the layer of the TiO₂ NPs at pH 5.0.

antisymmetric $\nu_{\text{as}}(\text{COO})$ vibration [25], respectively. The energy difference between the two vibrations is $\Delta\nu_{\text{as-s}}(\text{ionic}) = 135 \text{ cm}^{-1}$. Fig. 5B shows the spectra obtained with the n-butyric acid solution in contact with the layer of P25 TiO_2 . We assign the peak at 1529 cm^{-1} to the $\nu_{\text{as}}(\text{COO})$ vibration which has been shifted by 20 cm^{-1} to lower frequency by the interaction with TiO_2 . This reduces the energy separation between $\nu_{\text{as}}(\text{COO})$ and $\nu_{\text{s}}(\text{COO})$ from 135 cm^{-1} to $\Delta\nu_{\text{as-s}}(\text{ads}) = 119 \text{ cm}^{-1}$. Comparing $\Delta\nu_{\text{as-s}}(\text{ads})$ with $\Delta\nu_{\text{as-s}}(\text{ionic})$ allows distinguishing between different bonding modes for carboxylates on the substrates [16,26]. In the case of $\Delta\nu_{\text{as-s}}(\text{ads}) < \Delta\nu_{\text{as-s}}(\text{ionic})$ here, the carboxylate is bound with the bridging or chelating bidentate structure [16,26]. In the case of bridging structure, the two oxygen atoms of butyrate are, respectively, linked to two reactive centers on the TiO_2 , forming a five-membered ring which appends to the TiO_2 surface.

For the purpose of comparison, aqueous solutions of acetic acid are also subjected to the ATR-FTIR analysis with respect to the carboxylate. From the spectra shown in Fig. 6, it is observed that $\nu_{\text{as}}(\text{COO})$ shifts by 25 cm^{-1} to a lower frequency of 1510 cm^{-1} as a result of the interaction with TiO_2 . This reduces the energy separation between $\nu_{\text{as}}(\text{COO})$ and $\nu_{\text{s}}(\text{COO})$ from 136 cm^{-1} (ionic) to 90 cm^{-1} (ads), being similar to the results by other authors [16]. On comparison, we find that at each concentration of the solutions, $\nu_{\text{as}}(\text{COO})$ band of the adsorbed butyrate overwhelms that of the ionic butyrate (Fig. 5B), but a contrary behavior occurs for acetate (Fig. 6B). With the concentration increasing, the ratio of adsorbed $\nu_{\text{as}}(\text{COO})$ to ionic $\nu_{\text{as}}(\text{COO})$ increases for the butyric acid solution but decreases for the acetic acid solution. Taking $\nu_{\text{as}}(\text{COO})$ of the ionic carboxylate as the reference, we obtain that n-butyrate adsorbs on the TiO_2 more strongly than acetate in the solutions. It is realized here that the decarboxylation was suggested to associate with the acetate bridged on the TiO_2 surface. In brief, hole transfer to the five-membrane ring results in cleavage at the β -carbon position [12]. If so, the difference in photocatalytic efficiencies between butyric acid and acetic acid can be explained in term of carboxylate adsorption. We believe the weaker adsorption of acetate is due to a strong trend of dimerization for acetic acid by hydrogen bonding [27].

There are spectral variations for the unionized carboxylic acid. The broad band at 1278 cm^{-1} (Fig. 6), which is assigned to the $\nu(\text{COH})$ vibration of the carboxylic group of acetic acid [16], bulges on the low frequency side and seems to resolve into three peaks when the acetic acid solution contacts with the TiO_2 . This indicates the interactions of several types between the carboxylic group and TiO_2 surface. In addition to the obvious hydrogen bonding, the positively charged $>\text{TiOH}_2^+$ formed under $\text{pH} < \text{pH}_{\text{zpc}}$ should be taken into account, as the $\nu(\text{COH})$ band can be shifted visibly when imposed by charged species [16]. The bands in the region of $1150\text{--}1365 \text{ cm}^{-1}$ (Fig. 5) are attributed to the hydroxyl or C–O vibration of the carboxylic group in butyric acid. The major variation observed consists in that the bands at ca. 1264 and 1350 cm^{-1} are intensified as a result of the interaction, while the peak broadening and splitting to certain degree appear. It is emphasized that the two bands are not new because they also appear at the neat butyric acid solution despite of their weakness. It is mentioned here that theoretical calculations on pyruvic acid have identified two conformers of the molecules with distinguished enthalpy energies [28]. For this reason, we suggest that the pair of bands at ca. 1212 and 1310 cm^{-1} in this region would be attributed to the conformer of butyric acid that is the most stable in aqueous solution, while the bands at 1264 and 1350 cm^{-1} would refer to another conformer that is preferably adsorbed on the TiO_2 NPs.

4. Conclusions

The photopolymerizations of vinyl acetate are obtained by adding propionic acid, n-butyric acid and pivalic acid, respectively, into the aqueous suspension consisting of the TiO_2 nanoparticles and vinyl acetate. It is demonstrated by ^{13}C NMR that the polymerization of vinyl acetate is initiated by n-propyl radicals that are generated from the decarboxylation of butyric acid. The universal reaction mechanism is thus established with extending the photo-Kolbe reaction from acetic acid to the carboxylic acids with longer chains. In order to better understand the decarboxylation reaction, the polymerizations using sodium n-butyrate are carried out, and the obtained results clearly testify that the carboxylate anions participate into the photocatalyzed decarboxylation. According to the ^{13}C NMR data obtained for the synthesized PVAc, it is drawn that n-butyric acid performs higher initiation-rate than acetic acid. The analysis based on the free radical polymerization kinetics indicates that the decarboxylation of butyric acid is more efficient than acetic acid in their aqueous solutions. The ATR-FTIR spectra are acquired with the aqueous solutions of the carboxylic acids in contact with a layer of the TiO_2 nanoparticles. The results correlate the decarboxylation efficiency with the adsorption intensity of the carboxylates on TiO_2 surface, and have direct implications to further study of the extended photo-Kolbe reactions.

Acknowledgements

We thank National Nature Science Foundation of China (NSFC) for financial support of this research (20574011). Science and Technology Commission of Shanghai Municipality is greatly appreciated for financial supports (0752nm006, 055207080).

References

- [1] M.R. Hoffman, S.T. Martin, W. Choi, D.W. Bahnemann, Chem. Rev. 95 (1995) 69–96.
- [2] A.J. Hoffman, G. Mills, H. Yee, M.R. Hoffman, J. Phys. Chem. 96 (1992) 5540–5546.
- [3] A.L. Stroyuk, V.M. Granchak, A.V. Korzhak, S.Y. Kuchmii, J. Photochem. Photobiol. A: Chem. 162 (2003) 339–351.
- [4] X.Y. Ni, J. Ye, C. Dong, J. Photochem. Photobiol. A: Chem. 181 (2006) 19–27.
- [5] C. Dong, X.Y. Ni, J. Macromol. Sci. A: Pure Appl. Chem. 41 (2004) 547–563.
- [6] J. Ye, X.Y. Ni, J. Macromol. Sci. A: Pure Appl. Chem. 42 (2005) 1451–1461.
- [7] D. Yang, X.Y. Ni, Z. Weng, W.K. Chen, J. Photochem. Photobiol. A: Chem. 195 (2008) 323–329.
- [8] B. Kraeutler, A.J. Bard, J. Am. Chem. Soc. 100 (1978) 2239–2240.
- [9] B. Kraeutler, A.J. Bard, J. Am. Chem. Soc. 100 (1978) 5985–5992.
- [10] T. Sakata, T. Kawai, K. Hashimoto, J. Phys. Chem. 88 (1984) 2344–2350.
- [11] Y. Nosaka, M. Kishimoto, J. Nishino, J. Phys. Chem. B 102 (1998) 10279–10283.
- [12] M.A. Henderson, J.M. White, B.H. Uetsuka, H. Onish, J. Am. Chem. Soc. 125 (2003) 14974–14975.
- [13] S. Sato, K. Ueda, Y. Kawasaki, R. Nakamura, J. Phys. Chem. B 106 (2002) 9045–9047.
- [14] M.I. Franch, J.A. Ayllón, J. Peral, X. Domènech, Catal. Today 76 (2002) 221–233.
- [15] S.J. Hug, B. Sulzberger, Langmuir 10 (1994) 3587–3597.
- [16] F.P. Rotzinger, J.M. Kesselman-Truttmann, S.J. Hug, V. Shklover, M. Graetzel, J. Phys. Chem. B 108 (2004) 5004–5017.
- [17] G. Sivalingam, R. Karthik, G. Madras, Ind. Eng. Chem. Res. 42 (2003) 3647–3653.
- [18] D. Britton, F. Heatley, P.A. Lovell, Macromolecules 31 (1998) 2828–2837.
- [19] L.P. Lindeman, J.Q. Adams, Anal. Chem. 43 (1971) 1245–1252.
- [20] T. Shiono, S.M. Azad, T. Ikeda, Macromolecules 32 (1999) 5723–5727.
- [21] E. Breitmaier, W. Voelter, ^{13}C -NMR Spectroscopy, 2nd ed., Verlag Chem. ie, 1978.
- [22] J.P. Fouassier, Photoinitiation, Photopolymerization and Photocuring, Hanser, Munich, 1995.
- [23] G. Odian, Principle of Polymerization, 3rd ed., Wiley-Interscience, 1991.
- [24] J. Smid, M. Szwarc, Am. Chem. Soc. 79 (1956) 1534–1537.
- [25] S.E. Cabaniss, I.F. McVey, Spectrochim. Acta Part A 51 (1995) 2385–2395.
- [26] G.B. Deacon, F. Huber, R.J. Phillips, Inorg. Chim. Acta 104 (1985) 41–45.
- [27] Y.A. Elabd, T.A. Barbari, Ind. Eng. Chem. Res. 40 (2001) 3076–3084.
- [28] I.D. Reva, S.G. Stepanian, L. Adamowicz, R. Fausto, J. Phys. Chem. A 105 (2001) 4773–4780.